



# Human Mixed-Lineage Leukemia, Translocated to 1 (MLLT1)



## A Target Enabling Package (TEP)

Gene ID / UniProt ID	<a href="#">4298 / Q03111</a>
Target Nominator	Pharma partner
SGC Authors	Thomas Christott, Moses Moustakim, James Bennett, Carmen Coxon, Octovia Monteiro, Charline Giroud, Paul E Brennan, Oleg Fedorov
Collaborating Authors	N/A
Target PI	Dr Oleg Fedorov (SGC Oxford)
Therapeutic Area(s)	Cancer (Acute Myeloid Leukaemia)
Disease Relevance	Has been shown to be required for disease maintenance in acute myeloid leukaemia.
Date Approved by TEP Evaluation Group	June 13 <sup>th</sup> 2018
Document version	2
Document version date	October 2020
Citation	<a href="https://doi.org/10.5281/zenodo.2556640">https://doi.org/10.5281/zenodo.2556640</a>
Affiliations	N/A

We respectfully request that this document is cited using the DOI value as given above if the content is used in your work.

### USEFUL LINKS



Open Targets



(Please note that the inclusion of links to external sites should not be taken as an endorsement of that site by the SGC in any way)

### SUMMARY OF PROJECT

Overexpression of MLLT1 (also known as ENL, LTG19 and YEATS1) has recently been implicated as a driver of acute myeloid leukaemia (AML)(1, 2). Its epigenetic reader domain (dubbed YEATS domain) links histone acylation to gene expression via its role in the super elongation complex (SEC) (3) and its interaction with the histone methyl transferase DOT1L. Since epigenetic readers have been shown to be tractable targets for small molecule inhibitors, we have performed a library screen using a peptide displacement assay to identify inhibitors of MLLT1 interaction with acetylated histone tails. The screen yielded a potent hit and in further characterisation with biophysical methods it displayed a sub-micromolar  $K_D$  for MLLT1 and its paralog MLLT3 (Also known as AF9) with no detectable binding to two other human YEATS proteins.

## SCIENTIFIC BACKGROUND

MLLT1 contains an epigenetic reader domain (dubbed the YEATS domain), which recognises acylated lysine residues on histone 3, mainly acetyl lysine. MLLT1 had until recently been recognised only as a fusion partner for the transcriptional co-activator MLL1 in MLL1 rearranged mixed lineage leukaemia (MLL). There, the oncogenic function of MLLT1 is to link MLL1 with the super elongation complex and the histone methyl transferase DOT1L which drives the dysregulation of multiple genes(3–7).

However, there is now mounting evidence that the overexpression of MLLT1 is a driver in non-MLLT1 rearranged acute myeloid leukaemia (AML) by directly linking the epigenetic readout via YEATS domain to the oncogenic dysregulation of gene expression (1, 2).

CRISPR/Cas9 driven knockout of MLLT1 has been shown to significantly reduce cell proliferation and invasiveness of AML cell lines *in vitro* and in mouse xenograft models. Subsequent rescue with ectopically expressed native MLLT1 restored the disease phenotype while rescue with mutants that are deficient in the binding pocket with which MLLT1 recognises acyl lysine residues was unable to restore the phenotype (1). Similarly, targeting tagged MLLT1 for degradation with the dTAG system (8) also perturbed the disease phenotype (2).

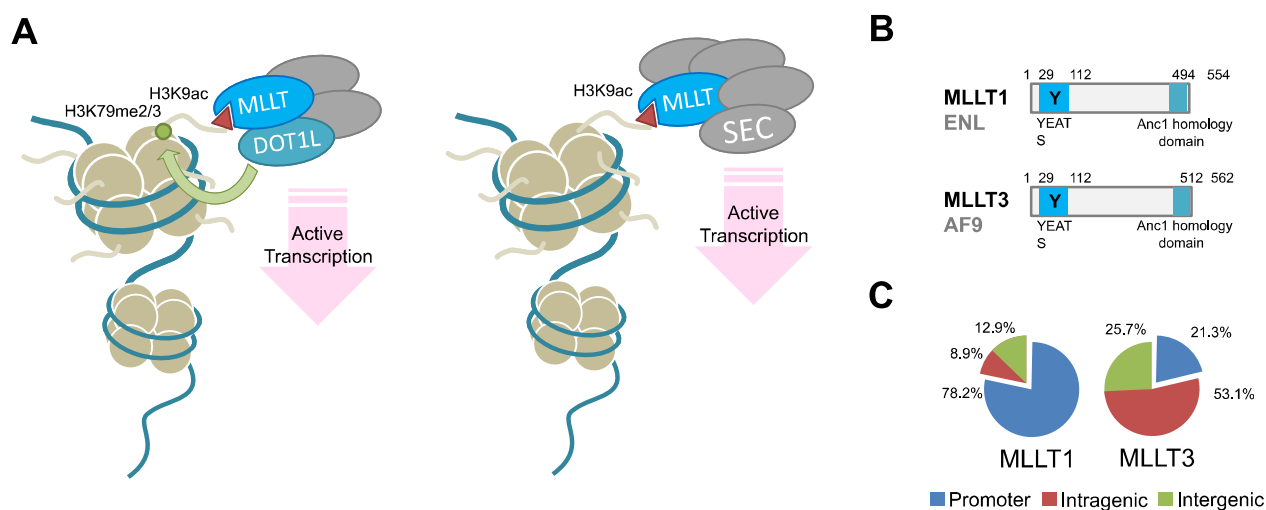


**Figure 1:** (A) Function of MLLT1/MLLT3 in gene transcription (MLLT: MLLT1 or MLLT3; SEC: Super elongation complex). (B) Domain structure (C) Genomic distribution of MLLT1 and MLLT3 (1, 9)

## RESULTS – THE TEP

### Protein Production

Using the methods described below, we were able to express the YEATS domains of all four human YEATS domain containing proteins (MLLT1, MLLT3, YEATS2, YEATS4) in quantities and at purities sufficient for screening campaigns with only two chromatography steps. For MLLT1, MLLT3 and YEATS4, the use of C-terminal His tags is highly preferable for yield, purity and protein stability. 12 litre expression cultures in standard TB medium yielded between 20 – 50 mg protein.

## Screening and Hit Characterisation

Several libraries were screened for compounds that inhibit the binding of MLLT1 to the histone peptide using an AlphaScreen® assay. A number of hits were re-purchased and re-characterisation via full dose response experiments, DSF and ITC. One compound was identified which possessed single-digit micromolar activity in the AlphaScreen® assay and sub-micromolar  $K_D$  in ITC (**Figure 2**)(10).

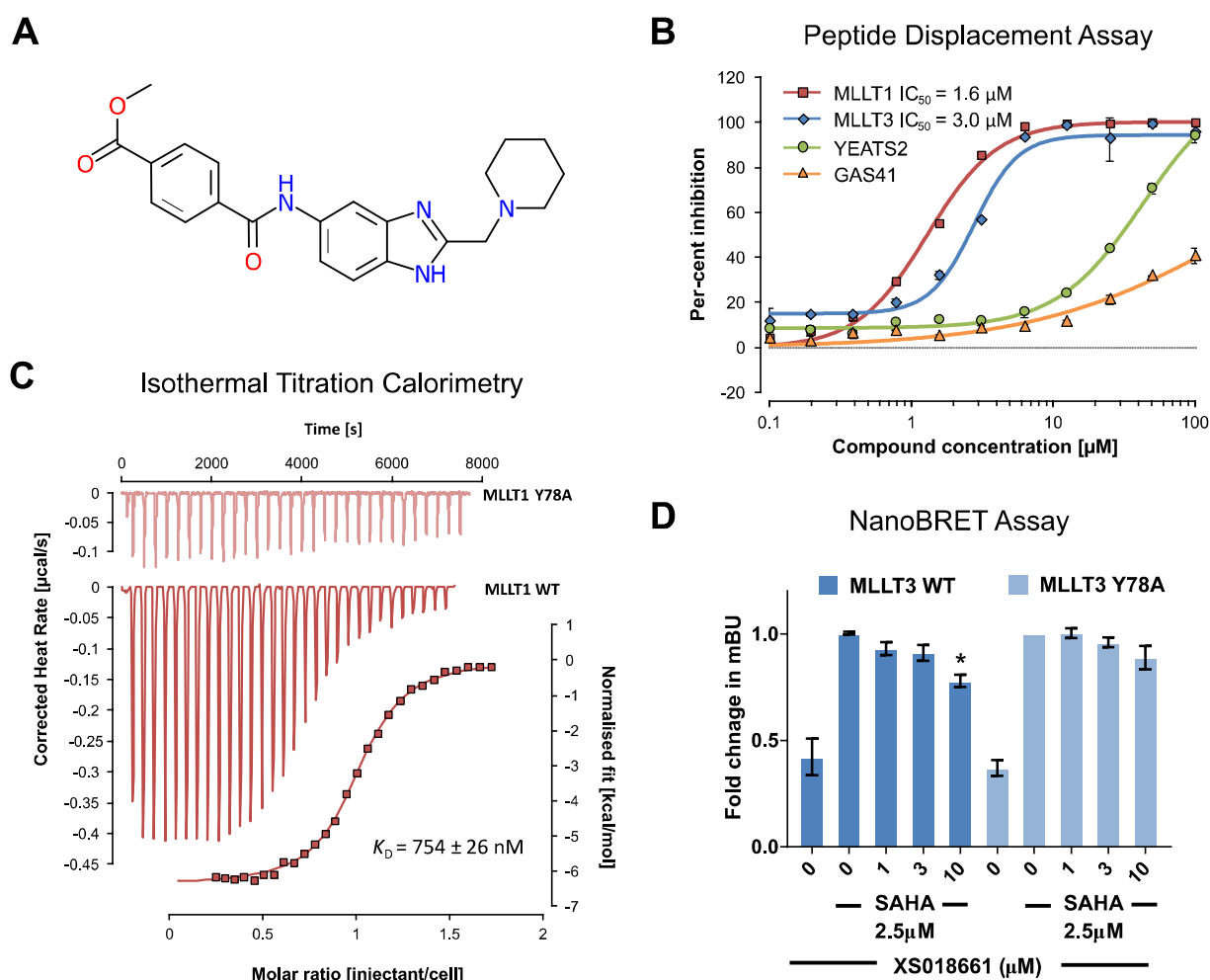


**Figure 2:** (A) Structure of the initial library screen hit (B) AlphaScreen® dose response curves with all four human YEATS domains and (C) Isothermal titration calorimetry of the initial library screen hit against MLLT1 WT and MLLT1Y78A. (D) NanoBRET assay with wild type and mutant MLLT3. Bar chart represents fold change in mBU NanoBRET showing the displacement of N-terminal-nanoLuc-MLLT3 WT or N-terminal-nanoLuc-MLLT3 Y78A from C-terminal HaloTag-H3.3 after 24h treatment with XS018661 (1-10  $\mu$ M) in the presence of 2.5  $\mu$ M SAHA.

	MLLT1	MLLT3	YEATS2	YEATS4
IC <sub>50</sub> ( $\mu$ M)	2.4	7.3	> 200	> 200
$\Delta T_M$ ( $^{\circ}$ C)	2.4	4.5	0.5	0.1
$K_D$ (nM)	754	523	N/T	N/T
$\Delta G$ (kcal/mol)	-8.2	-8.5	-	-
$\Delta H$ (kcal/mol)	-6.4	-7.6	-	-
$-T\Delta S$ (kcal/mol)	-1.8	-0.9	-	-

**Table 1:** Biophysical characterisation of the library hit (N/T: Not tested)

## Hit Optimisation and Chemical Probe Development

Using a poised approach to ligand design, the original hit was disconnected into three synthons and rapidly diversified using readily available precursors. After several rounds of synthesis, a compound with  $\sim 100$  nM  $K_D$  for both MLLT1 and MLLT3 was developed (**Figure 3**)(11).

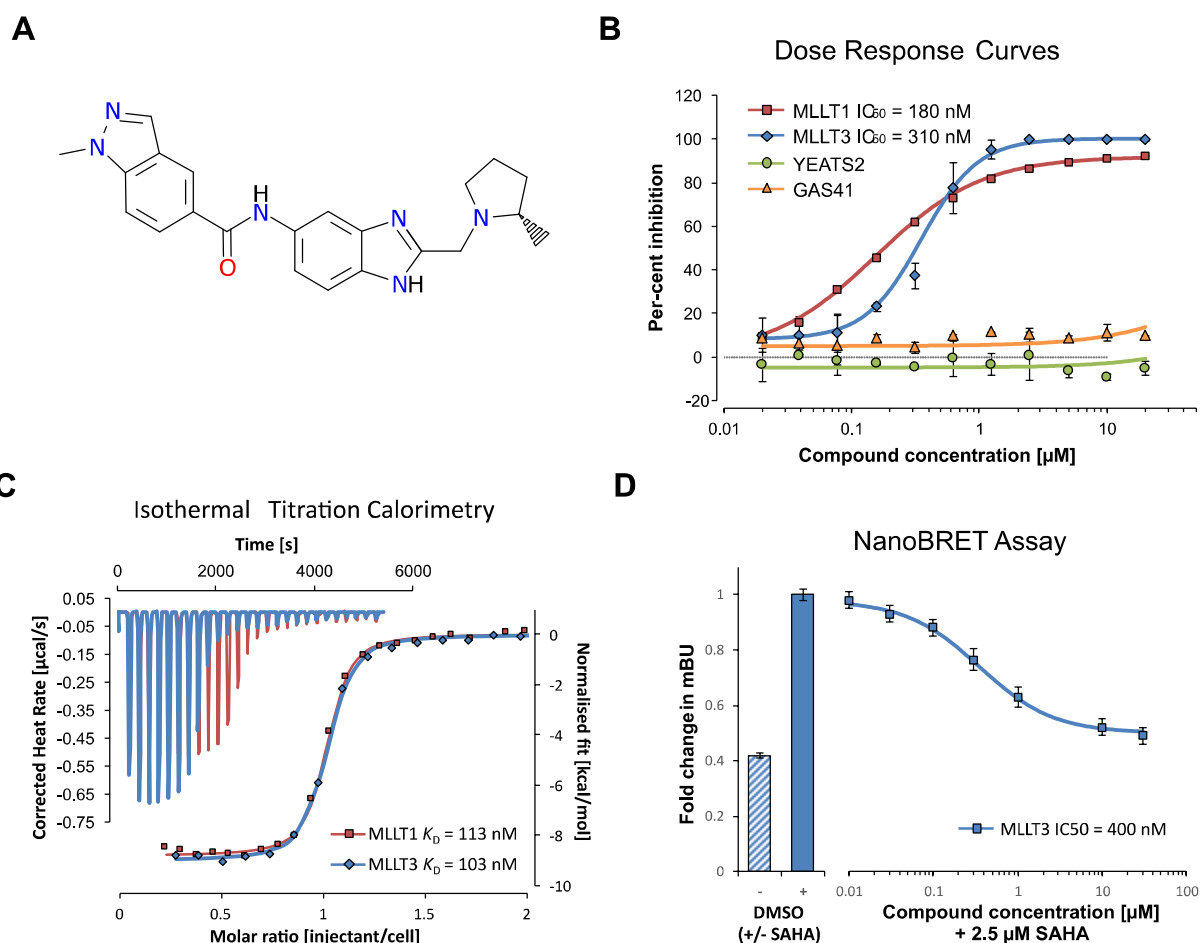


**Figure 3:** (A) Structure of SGC-iMLLT (B) AlphaScreen<sup>®</sup> dose response curves with all four human YEATS domains and (C) Isothermal titration calorimetry of the initial library screen hit against MLLT1 WT and MLLT3 WT. (D) NanoBRET assay with wild type MLLT3. Chart represents fold change in mBU NanoBRET showing the displacement of N-terminal-nanoLuc-MLLT3 WT from C-terminal HaloTag-H3.3 after 24h treatment with XS018661 (0.01-30  $\mu$ M) in the presence of 2.5  $\mu$ M SAHA.

	MLLT1	MLLT3	YEATS2	YEATS4
$IC_{50}$ (nM)	180	310	> 200	> 200
$\Delta T_M$ ( $^{\circ}$ C)	4.0	3.5	0.5	0.5
$K_D$ (nM)	113	103	N/T	N/T
$\Delta G$ (kcal/mol)	-9.4	-9.5	-	-
$\Delta H$ (kcal/mol)	-8.8	-9.0	-	-
$-\Delta S$ (kcal/mol)	-0.6	-0.5	-	-

**Table 2:** Biophysical characterisation of SGC-iMLLT (N/T: Not tested)

## Structural Data

The structures of the MLLT1 YEATS domain with two inhibitors generated were solved and deposited into the PDB (**Table 3**). SGC-iMLLT was shown to occupy the acyllysine binding site previously identified in the literature, making a number of contacts

PDB ID	Structure Details
6HT0	Crystal structure of MLLT1 (ENL) YEATS domain in complexed with compound 94
6HT1	Crystal structure of MLLT1 (ENL) YEATS domain in complexed with SGC-iMLLT (compound 92)

**Table 3:** Structures solved

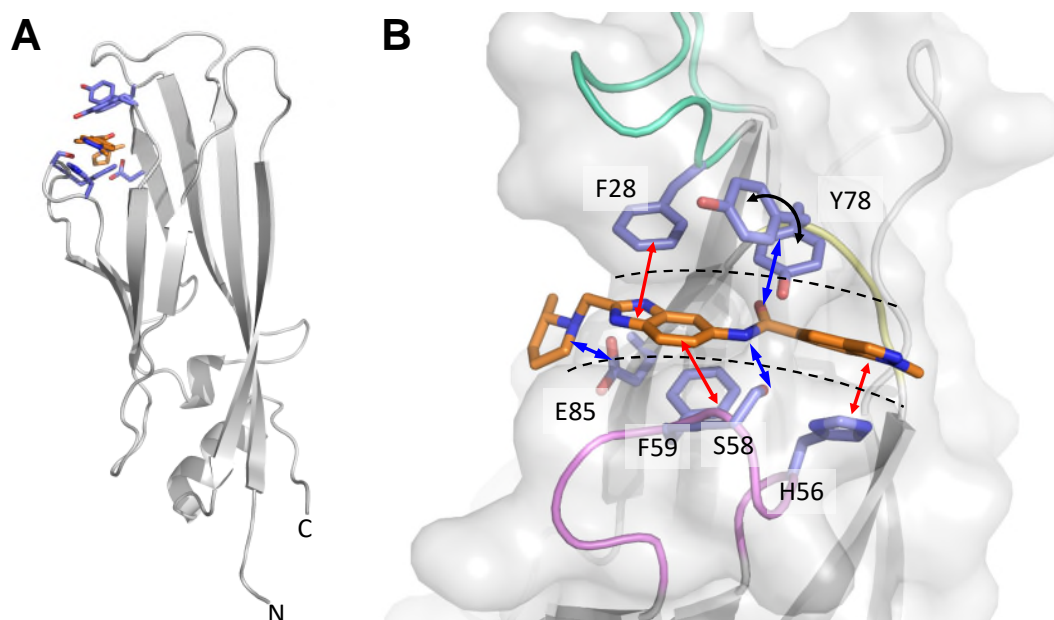


**Figure 4:** Structure of SGC-iMLLT bound to the YEATS domain of MLLT1 (6HT1) with compound contacting residues highlighted in blue. **(A)** Complete view, N- and C-termini marked. **(B)** Detail view of binding pocket. Blue arrows: hydrogen bonds between SGC-iMLLT and side-chains (E85, S58) and backbone (Y78); Red arrows:  $\pi$ - $\pi$  stacking of SGC-iMLLT and side chains (F28, F59, Y78, H56); Black arrow denotes “flipped” conformations of Y78.

## CONCLUSION

Here, we show the discovery of a potent first in class chemical probe of a promising new target in MLL/AML biology. The assays we developed will aid the discovery, further characterisation and development of inhibitors for the wider YEATS family, most of which are implicated as key players in a number of different cancer types while the initial inhibitor will serve as a springboard for other researchers to accelerate their work in YEATS biology.

## FUNDING INFORMATION

The work performed at the SGC has been funded by a grant from the Wellcome [106169/ZZ14/Z] and the Innovative Medicines Initiative Joint Undertaking (IMI JU) under grant agreement [115766].

## ADDITIONAL INFORMATION

### Materials and Methods

#### Proteins Purified

All four human members of the YEATS domain (**Table 4**) were recombinantly expressed in *E. coli* BL21(DE3) cells upon induction with 0.4 mM IPTG and purified using standard protocols for centrifugal harvest. Cells were lysed via sonication and the lysate clarified via centrifugation. Immobilised metal affinity chromatography (IMAC) was performed with GE HisTrapFF columns (5 ml) to isolate target proteins from lysate, followed by size exclusion chromatography with GE HiLoad 16/60 Superdex 75pg columns. For buffer, 20-50 mM Tris at pH 7.5, 500 mM NaCl and 2 mM DTT were used, supplemented for IMAC with 20 mM imidazole for lysis and wash, and 300 mM imidazole for elution.

Protein	UniProtKB	Boundaries		6His tag
		Start	Stop	
MLLT1	Q03111	M1	M148	C-terminal
MLLT3	P42568	M1	A138	C-terminal
YEATS2	Q9ULM3	S202	E345	N-terminal
YEATS4	O95619	V16	K225	C-terminal

**Table 4:** Proteins purified for this TEP

#### Peptide Displacement Assay

Peptide displacement assays were set up with biotinylated peptides (chosen based on ChIPseq data from the literature and purchased from LifeTein, **Table 5**) and 6His tagged protein. For detection, two orthogonal technologies were used, *i.* AlphaScreen® technology from Perkin Elmer and *ii.* HTRF from Cisbio. Compounds were dispensed in duplicate at single concentration (100 µM) for the initial screen and as 11-point dose response curves starting from 200 µM for IC<sub>50</sub> value determination.

YEATS domain	Peptide shorthand	Position	Peptide sequence
MLLT1	H3K18ac	12-30	GGKAPR(K-acetyl)QLATKAARKSAPY(K-biotin)
MLLT3	H3K9ac	2-20	ARTKTAR(K-acetyl)STGGKAPRKQLY(K-biotin)
YEATS2	H3K27cro	15-32	biotin-GKPRKQLATAAR(K-crotonyl)SAPAT
YEATS4	H3K27cro	15-32	biotin-GKPRKQLATAAR(K-crotonyl)SAPAT

**Table 5:** Peptides used for the peptide displacement assays

To determine optimal assay conditions for each protein prep, proteins and peptides were titrated against each other in a 16 by 16 matrix in 1:1 dilutions, starting from 3.2 µM. For the final ratio of protein and peptide to use in the assay, the point representing the EC<sub>90</sub> in the two-dimensional titration was chosen. Typically, final assay concentrations for protein and peptide fell between 25 and 200 nM. For AlphaScreen®, AlphaScreen Histidine (Nickel Chelate) Detection Kit donor and acceptor beads were used at a 1:2500 dilution from purchased stock; for HTRF, SA-XL665 and anti-6His antibody were used at 1:2000 and 1:10000 dilution from purchased stock, respectively. Assays were performed on 384 well ProxiPlates (Perkin Elmer) at a final volume of 20 µl and plates were read using a Pherastar FSX plate reader (BMG Labtech).

### Isothermal Titration Calorimetry

Isothermal titration calorimetry (ITC) was carried out using a TA NanoITC (standard volume) instrument. Protein was prepared by dialysis (overnight at 4°C) against a ~1000 times excess of buffer (20 mM Tris at pH 7.5, 500 mM NaCl, 5% (v/v) glycerol, 2 mM DTT) using SnakeSkin® Dialysis Tubing with a 7 kDa MWCO and then concentrated to 300 µM. The experiment was carried out at 20°C in reverse mode with the compound in the cell at 50 µM and the protein in the syringe at 300 µM due to the solubility of the compound with the first injection at 4 µl and the following 30 at 8 µl. Data was analysed using the NanoAnalyze software package by TA Instruments.

### Differential Scanning Fluorimetry

Differential scanning fluorimetry (DSF) to determine the effect of compounds on the thermal stability of proteins ( $\Delta T_m$ ) was carried out on 384 well PCR plates using a LightCycler 480 (Roche). Protein at 10 µM was buffered in 10 mM HEPES at pH 7.5 and 500 mM NaCl. The experiment was carried out from 25 to 95°C with three acquisitions per degree. Compounds were added at 50 µM final concentration and DMSO reference and no-addition controls were also collected.

### SAR by Catalogue and Lead Development

Additional compounds were purchased to perform 'SAR by catalogue'. The compounds were analysed in the peptide displacement assay and differential scanning fluorimetry as described above (**Figure 3, Table 6**).

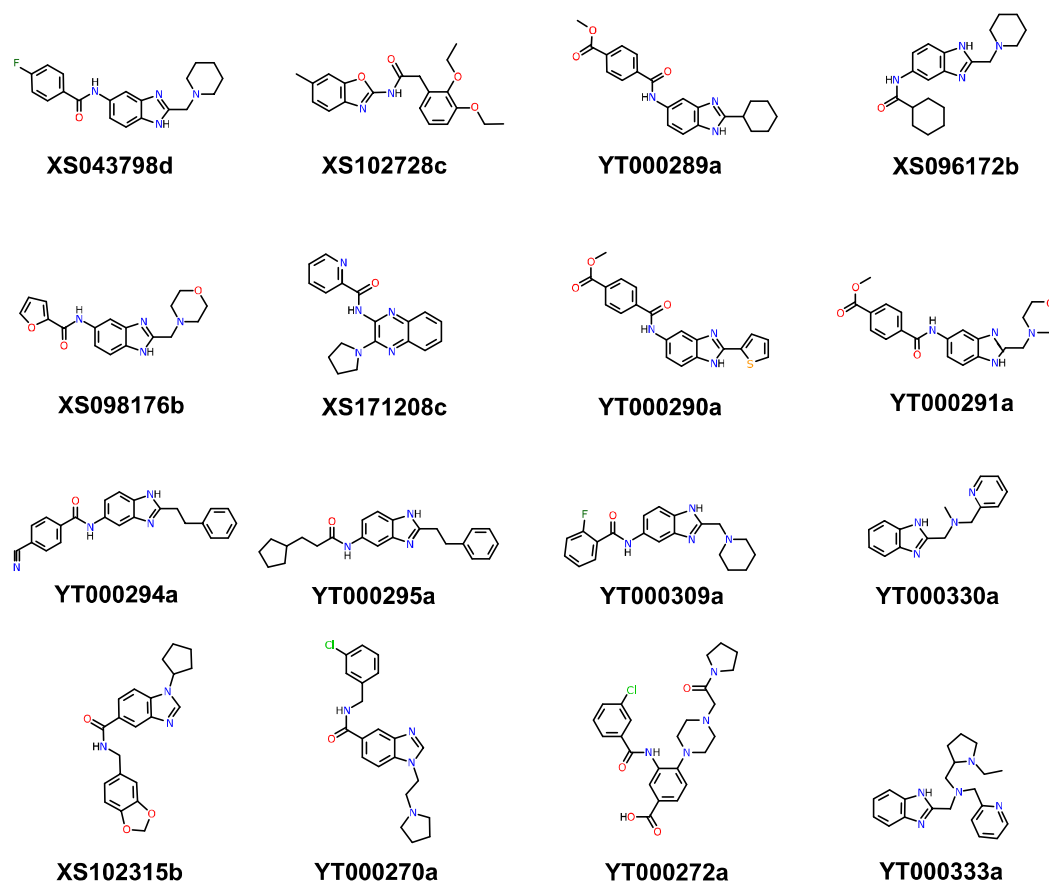


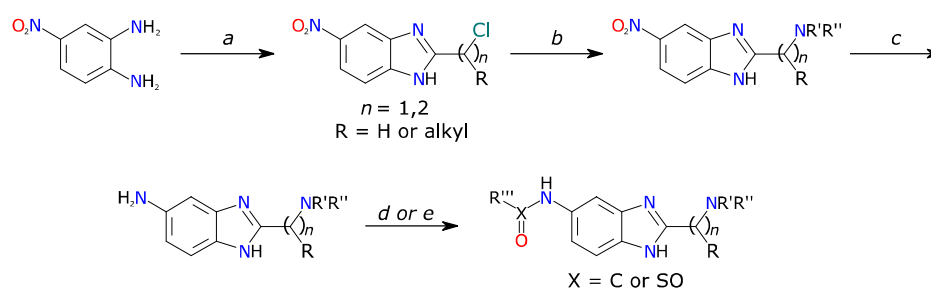
**Figure 5:** Structures of compounds purchased for 'SAR by catalogue'.

Compound	MLLT1		MLLT3		YEATS2		YEATS4	
	IC <sub>50</sub> [μM]	ΔT <sub>m</sub> [°C]	IC <sub>50</sub> [μM]	ΔT <sub>m</sub> [°C]	IC <sub>50</sub> [μM]	ΔT <sub>m</sub> [°C]	IC <sub>50</sub> [μM]	ΔT <sub>m</sub> [°C]
XS043798c	8.8	1.0	27.6	1.8	134.0	0.2	>200	0.0
XS043798d	7.1	1.2	>200	2.1	>200	0.2	>200	0.1
XS096172b	162.9	0.2	>200	0.4	>200	0.2	>200	0.0
XS098176b	49.9	0.0	>200	0.0	>200	0.2	>200	0.1
XS102315b	13.8	0.3	52.2	0.6	83.3	0.2	>200	0.1
XS102728c	18.0	0.2	51.8	0.0	18.6	0.2	>200	0.1
XS171208c	5.6	0.0	47.1	-0.1	6.7	0.2	44.0	-0.4
YT000270a	18.2	0.0	59.3	0.3	64.9	0.1	>200	0.1
YT000272a	43.8	0.0	70.1	0.1	33.9	0.1	>200	0.1
YT000289a	30.1	0.0	>200	0.3	>200	0.5	52.0	0.4
YT000290a	16.1	0.0	>200	0.6	>200	0.5	>200	1.4
YT000291a	19.3	0.3	>200	0.6	>200	0.5	>200	0.2
YT000294a	44.3	0.2	>200	1.0	>200	1.3	>200	1.1
YT000295a	>200	0.0	>200	0.6	>200	0.5	57.6	0.9
YT000309a	9.7	0.3	>200	0.6	>200	0.8	>200	1.1
YT000330a	0.7	-0.2	0.9	0.1	1.0	0.1	0.9	-0.3
YT000333a	26.4	0.0	>200	-0.1	>200	0.1	>200	0.1

**Table 6:** Results of peptide displacement assays and differential scanning fluorimetry assays with the compounds purchased for 'SAR by catalogue'.

## Chemistry

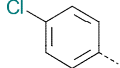
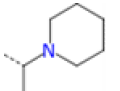
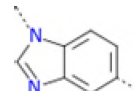
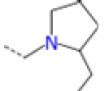
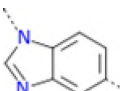
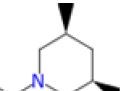
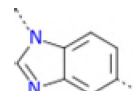
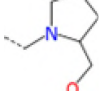
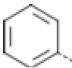
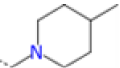
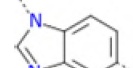
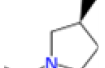
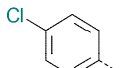
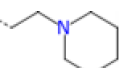
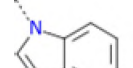
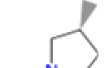
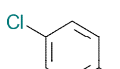
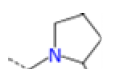
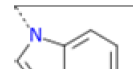
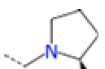
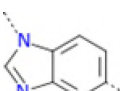
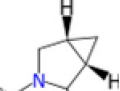
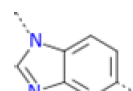
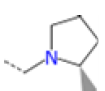
Substitutions in positions R1 and R2 around the central motif of the library screen hit (**Figure 6**) were performed and the resulting compounds tested in the peptide displacement assay (**Table 7**). Detailed information of chemical synthesis can be found in *Moustakim, Christott et al., 2018* (11)



**Figure 6:** Synthesis of the central motif of the library screen hit. **a** ethyl 2-chloroacetate (1.2 eq), 4N HCl (0.6 M), 16 h, 100°C, 4-95%; **b** amine (1.2-1.5 eq), Na<sub>2</sub>CO<sub>3</sub><sup>-</sup> (1.5 eq), 23°C, 3-82; **c** H<sub>2</sub> Pd/C (10%), 17-88%; **d** sulfonyl/acid chloride (1.2 eq), PS-DIPEA (2 eq), 16 h; **e** acid (1.2 eq), HATU (1.5 eq), PS-DIPEA (2 eq), 16 h, 8-100%.

For more information regarding any aspect of TEPs and the TEP programme, please contact [teps@thesgc.org](mailto:teps@thesgc.org)



	R1	R2	MLLT1 IC <sub>50</sub> [μM]		R1	R2	MLLT1 IC <sub>50</sub> [μM]
<b>81</b>			>20	<b>87</b>			0.3 ± 0.1
<b>82</b>			5.7 ± 2.4	<b>88</b>			0.97 ± 0.66
<b>83</b>			>20	<b>89</b>			0.35 ± 0.18
<b>84</b>			>20	<b>90</b>			0.52 ± 0.48
<b>85</b>			0.28 ± 0.02	<b>91</b>			2.3 ± 0.77
<b>86</b>			1.4 ± 0.86	<b>92</b>			<b>0.18 ± 0.1</b>

**Table 7:** Selected binding affinity characterisation data of benzimidazole series for MLLT1 YD

### NanoLuciferase Bioluminescent Resonance Energy Transfer (NanoBRET) Assay

Cellular activity against MLLT3 was assessed using a NanoBRET assay. HEK293 cell (8 x 10<sup>5</sup>) were plated in each well of a 6-well plate after 6h cells were co-transfected with C-terminal HaloTag-Histone 3.3 (NM\_002107) and an N-terminal NanoLuciferase fusion of MLLT3 (original MLLT3 WT sequences from Promega HaloTag<sup>®</sup> human ORF in pFN21A and MLLT3 MUT - Y78A Tyrosine is changed to an Alanine) at a 1:10 (NanoLuc<sup>®</sup> to HaloTag<sup>®</sup>) ratio respectively with FuGENE HD transfection reagent.

Sixteen hours post-transfection, cells were collected, washed with PBS, and exchanged into media containing phenol red-free DMEM and 4% FBS in the absence (control sample) or the presence (experimental sample) of 100 nM NanoBRET 618 fluorescent ligand (Promega). Cells were then re-plated in a 96-well assay white plate (Corning Costar #3917) at 2x10<sup>4</sup> cells per well. Compounds were then added directly to media (in the presence of SAHA 2.5 μM) at final concentrations 0-10 μM or an equivalent amount of DMSO as a vehicle control, and the plates were incubated for 24 h at 37°C in the presence of 5% CO<sub>2</sub>.

NanoBRET Nano-Glo substrate (Promega) was added to both control and experimental samples at a final concentration of 10 μM. Readings were performed within 10 minutes using a ClarioSTAR (BMG Labtech) equipped with 460 nm and 610 nm filters. A corrected BRET ratio was calculated and is defined as the ratio of the emission at 610 nm/460 nm for experimental samples minus the emission at 610 nm/460 nm for control samples (without NanoBRET fluorescent ligand). BRET ratios are expressed as millibRET units (mBU), where 1 mBU corresponds to the corrected BRET ratio multiplied by 1000.

## Crystallography

Crystallization was performed using protein at ~0.45 mM concentration and sitting drop vapor diffusion method at 20C. Co-crystals with compounds grew in various conditions containing either PEG3350 or PEG Smear Medium (12), of which other compositions were reported in the publications (11, 13). Alternatively, the inhibitor-complexed crystals were used for preparing seeds, which was then used for crystallization of apo crystals. Soaking was performed using fragments or inhibitors at ~5-40 mM. All crystals were cryo-protected with mother liquor supplemented with 25% ethylene glycol prior to flash-cooled in liquid nitrogen.

## References

1. Wan, L., Wen, H., Li, Y., Lyu, J., Xi, Y., Hoshii, T., Joseph, J. K., Wang, X., Loh, Y.-H. E., Erb, M. A., Souza, A. L., Bradner, J. E., Shen, L., Li, W., Li, H., Allis, C. D., Armstrong, S. A., and Shi, X. (2017) [ENL links histone acetylation to oncogenic gene expression in acute myeloid leukaemia](#). *Nature*. **543**, 265–269
2. Erb, M. A., Scott, T. G., Li, B. E., Xie, H., Paulk, J., Seo, H.-S., Souza, A., Roberts, J. M., Dastjerdi, S., Buckley, D. L., Sanjana, N. E., Shalem, O., Nabet, B., Zeid, R., Offei-Addo, N. K., Dhe-Paganon, S., Zhang, F., Orkin, S. H., Winter, G. E., and Bradner, J. E. (2017) [Transcription control by the ENL YEATS domain in acute leukaemia](#). *Nature*. **543**, 270–274
3. Yokoyama, A., Lin, M., Naresh, A., Kitabayashi, I., and Cleary, M. L. (2010) [A Higher-Order Complex Containing AF4 and ENL Family Proteins with P-TEFb Facilitates Oncogenic and Physiologic MLL-Dependent Transcription](#). *Cancer Cell*. **17**, 198–212
4. Mueller, D., Bach, C., Zeisig, D., Garcia-Cuellar, M. P., Monroe, S., Sreekumar, A., Zhou, R., Nesvizhskii, A., Chinnaiyan, A., Hess, J. L., and Slany, R. K. (2007) [A role for the MLL fusion partner ENL in transcriptional elongation and chromatin modification](#). *Blood*. **110**, 4445–4454
5. Mueller, D., García-Cuellar, M. P., Bach, C., Buhl, S., Maethner, E., and Slany, R. K. (2009) [Misguided transcriptional elongation causes mixed lineage leukemia](#). *PLoS Biol.* 10.1371/journal.pbio.1000249
6. Monroe, S. C., Jo, S. Y., Sanders, D. S., Basrur, V., Elenitoba-Johnson, K. S., Slany, R. K., and Hess, J. L. (2011) [MLL-AF9 and MLL-ENL alter the dynamic association of transcriptional regulators with genes critical for leukemia](#). *Exp. Hematol.* **39**, 77–86.e5
7. Biswas, D., Milne, T. A., Basrur, V., Kim, J., Elenitoba-Johnson, K. S. J., Allis, C. D., and Roeder, R. G. (2011) [Function of leukemogenic mixed lineage leukemia 1 \(MLL\) fusion proteins through distinct partner protein complexes](#). *Proc. Natl. Acad. Sci.* **108**, 15751–15756
8. Nabet, B., Roberts, J. M., Buckley, D. L., Paulk, J., Dastjerdi, S., Yang, A., Leggett, A. L., Erb, M. A., Lawlor, M. A., Souza, A., Scott, T. G., Vittori, S., Perry, J. A., Qi, J., Winter, G. E., Wong, K.-K., Gray, N. S., and Bradner, J. E. (2018) [The dTAG system for immediate and target-specific protein degradation](#). *Nat. Chem. Biol.* 10.1038/s41589-018-0021-8
9. Li, Y., Wen, H., Xi, Y., Tanaka, K., Wang, H., Peng, D., Ren, Y., Jin, Q., Dent, S. Y. R., Li, W., Li, H., and Shi, X. (2014) [AF9 YEATS domain links histone acetylation to DOT1L-mediated H3K79 methylation](#). *Cell*. **159**, 558–571
10. Christott, T., Bennett, J., Coxon, C., Monteiro, O., Giroud, C., Beke, V., Felce, S. L., Gamble, V., Gileadi, C., Poda, G., Al-awar, R., Farnie, G., and Fedorov, O. (2018) [Discovery of a Selective Inhibitor for the YEATS Domains of ENL/AF9](#). *SLAS Discov. Adv. Life Sci. R&D*.
11. Moustakim, M., Christott, T., Monteiro, O. P., Bennett, J., Giroud, C., Ward, J., Rogers, C. M., Smith, P., Panagakou, I., Saez, L. D., Ling, S., Gamble, V., Gileadi, C., Halidi, N., Heidenreich, D., and Chaikuad, A. (2018) [Discovery of an MLLT1 / 3 YEATS Domain Chemical Probe](#). *Angew. Chemie - Int. Ed.*
12. Chaikuad, A., Knapp, S., and Von Delft, F. (2015) [Defined PEG smears as an alternative approach to enhance the search for crystallization conditions and crystal-quality improvement in reduced screens](#). *Acta Crystallogr. Sect. D Biol. Crystallogr.* **71**, 1627–1639
13. Heidenreich, D., Moustakim, M., Schmidt, J., Merk, D., Brennan, P. E., Fedorov, O., Chaikuad, A., and Knapp, S. (2018) [A structure-based approach towards identification of inhibitory fragments for eleven-nineteen-leukemia protein \(ENL\)](#). *J. Med. Chem.*
14. Ni, X., Heidenreich, D., Christott, T., Bennett, J., Moustakim, M., Brennan, P. E., Fedorov, O., Knapp, S., and Chaikuad, A. (2019) [Structural insights into interaction mechanisms of alternative piperazine-urea](#)

YEAS domain binders in MLLT1. *ACS Med. Chem. Lett.*

## TEP IMPACT

We respectfully request that this document is cited using the DOI value as given above if the content is used in your work.